

Supporting Information

Samel et al. 10.1073/pnas.1120968109

SI Materials and Methods

Partial Purification of Cse4. A histone purification from cells carrying 3xHA-tagged Cse4 (AEY2781) was performed as previously described (1) with the following modifications. The DNA of extracts prepared from 6,000 OD cells was precipitated with 0.4 N HCl. After the ultrafiltration of the supernatant through an Amicon Ultra 100K column, the eluate was concentrated to 2 mL with Amicon Ultra 10K, lyophilized, and fractionated for 94 min by reversed-phase HPLC on an Agilent Zorbax 300SB-C3 column between 35% and 53% acetonitrile (ACN) (vol/vol) in 0.1% trifluoroacetic acid at 1 mL/min. Cse4-containing fractions were identified by dot blot, lyophilized, and used for SDS/PAGE.

Gel Electrophoresis of Cse4 and In-Gel Digestion. Cse4 from histone purifications was separated by SDS/PAGE. The gel was stained with Coomassie Blue using the Colloidal Blue Staining Kit (Sigma). The Cse4 band was excised and digested in-gel with trypsin (Promega) essentially as previously described (2). Briefly, the gel band was washed four times with 50 mM ammonium bicarbonate/50% ethanol (vol/vol) and incubated with 10 mM DTT in 50 mM ammonium bicarbonate for 1 h at 56 °C for protein reduction. An alkylation step was performed by incubating the sample with 55 mM iodoacetamide in 50 mM ammonium bicarbonate for 1 h at 25 °C in the dark. Gel pieces were washed twice with 50 mM ammonium bicarbonate, 50% ACN, dehydrated with 100% ethanol, and dried in a vacuum concentrator. Digestion was performed using 12.5 ng/mL trypsin in 50 mM ammonium bicarbonate for 16 h at 37 °C. The supernatant was transferred to a fresh tube, and the remaining peptides were extracted by incubating the gel pieces twice with 30% ACN in 3% trifluoroacetic acid (TFA), followed by dehydration with 100% ACN. The extracts were combined, reduced in volume in a vacuum concentrator, desalted, and concentrated using RP-C₁₈ StageTip columns. The eluted peptides were used for subsequent mass spectrometric analysis (3).

MS Analysis (Liquid Chromatography-MS/MS). Peptide mixtures were separated by nano-liquid chromatography (LC)-MS/MS using an Agilent 1100 Series nanoflow LC system (Agilent Technologies), interfaced to a 7-Tesla LTQ-FT-Ultra mass spectrometer (ThermoFisher Scientific). The nanoliter flow LC was operated in one column setup with a 15-cm analytical column (75- μ m inner diameter, 350- μ m outer diameter) packed with C18 resin (ReproSil, Pur C18AQ 3 μ m; Dr. Maisch HPLC GmbH). Solvent A was 0.1% formic acid (FA) and 5% ACN in ddH₂O, and solvent B was 95% ACN with 0.1% FA. Samples were injected in an aqueous 0.1% TFA solution at a flow rate of 500 nL/min. Peptides were separated with a gradient of 0–40% solvent B over 90 min followed by a gradient of 40–60% for 10 min and 60–80% over 5 min at a flow rate of 250 nL/min. The mass spectrometer was operated in a data-dependent mode to automatically switch between MS and MS/MS acquisition. In the LTQ-FT full scan, MS spectra were acquired in a range of m/z 300–1,350 by Fourier transform ion cyclotron resonance (FTICR) with resolution $r = 100,000$ at m/z 400 with a target value of 2,000,000. The five most intense ions were isolated for fragmentation in the linear ion trap using collision-induced dissociation at a target value of

5,000. Singly charged precursor ions were excluded. In the MS/MS method a dynamic exclusion of 60 s was applied, and the total cycle time was \sim 2 s. The nanoelectrospray ion source (Proxeon) was used with a spray voltage of 2.4 kV. No sheath and auxiliary gasses were used, and capillary temperature was set to 180 °C. Collision gas pressure was 1.3 millitorrs, and normalized collision energy using wide-band activation mode was 35%. Ion selection threshold was 250 counts with an activation $q = 0.25$. The activation time of 30 ms was applied in MS2 acquisitions.

Data Analysis and Sequence Assignment Using MASCOT. The raw data from LTQ-FT Ultra were converted to mgf files using Raw2MMSM software (4). MS/MS peak lists were filtered to contain at most six peaks per 100-Da intervals and searched by Mascot Daemon (version 2.2.2; Matrix Science) against a concatenated forward and reversed version of the yeast ORF database (*Saccharomyces* Genome Database at Stanford University; www.yeastgenome.org) (5, 6). This database was complemented with frequently observed contaminants (porcine trypsin, achromobacter lyticus lysyl endopeptidase, and human keratins) as well as with their reversed sequences. Search parameters were as follows: an initial MS tolerance of 7 ppm, a MS/MS mass tolerance at 0.5 Da, and full trypsin cleavage specificity, allowing for up to two missed cleavages. Carbamidomethylation of cysteine was set as a fixed modification, and variable modifications included mono- and dimethylation on lysine and arginine residues, trimethylation on lysines, oxidation on methionine, and acetylation on the N terminus of proteins. We accepted peptides and proteins with a false discovery rate of less than 1%, estimated according to the number of accepted reverse hits (5). Filtered data were then manually confirmed using the Qual Browser version 2.0.7 (ThermoFisher Scientific). Extracted ion chromatograms were constructed for precursor ions with mass tolerance of 10 ppm and mass precision up to four decimal places. Peak areas for both unmodified and modified peptide species were measured within the same retention time interval. In the case of the LAGDQQSINDR (27-37) peptide from the Cse4 protein, the relative abundance (%) of the modification was estimated from the relative proportion between two peptide species identified (me0 and me1).

Chromatin Immunoprecipitation. ChIP and quantitative real-time PCR were performed as previously described (7). Primer sequences are available upon request.

Chromosome Loss Assay. Generation of WT and mutant centromere-containing chromosome fragments was carried out as previously described (8). Briefly, plasmids containing WT and mutant CEN6-CDEI sequence (pAE1769, pAE1768) were linearized with NotI and used to transform *ade2-101* diploid strains (AEY7, AEY5005) to uracil prototrophy to generate a large, nonessential chromosome fragment carrying *URA3* and *SUP11* fused to the left arm of chromosome III. The transformants were restreaked on full medium to identify pink derivatives. Chromosome loss was monitored by the loss of the *SUP11* gene, which suppresses the *ade2* mutation, and whose absence thus causes a red pigmentation of the cells.

1. Waterborg JH (2000) Steady-state levels of histone acetylation in *Saccharomyces cerevisiae*. *J Biol Chem* 275:13007–13011.
2. Shevchenko A, Tomas H, Havlis J, Olsen JV, Mann M (2006) In-gel digestion for mass spectrometric characterization of proteins and proteomes. *Nat Protoc* 1:2856–2860.

3. Rappsilber J, Mann M, Ishihama Y (2007) Protocol for micro-purification, enrichment, pre-fractionation and storage of peptides for proteomics using StageTips. *Nat Protoc* 2:1896–1906.
4. Olsen JV, et al. (2005) Parts per million mass accuracy on an Orbitrap mass spectrometer via lock mass injection into a C-trap. *Mol Cell Proteomics* 4:2010–2021.

5. Elias JE, Haas W, Faherty BK, Gygi SP (2005) Comparative evaluation of mass spectrometry platforms used in large-scale proteomics investigations. *Nat Methods* 2:667–675.
6. Käll L, Storey JD, MacCoss MJ, Noble WS (2008) Assigning significance to peptides identified by tandem mass spectrometry using decoy databases. *J Proteome Res* 7: 29–34.

7. Weber JM, Irlbacher H, Ehrenhofer-Murray AE (2008) Control of replication initiation by the Sum1/Rfm1/Hst1 histone deacetylase. *BMC Mol Biol* 9:100.
8. Hegemann JH, Shero JH, Cottarel G, Philippsen P, Hieter P (1988) Mutational analysis of centromere DNA from chromosome VI of *Saccharomyces cerevisiae*. *Mol Cell Biol* 8: 2523–2535.

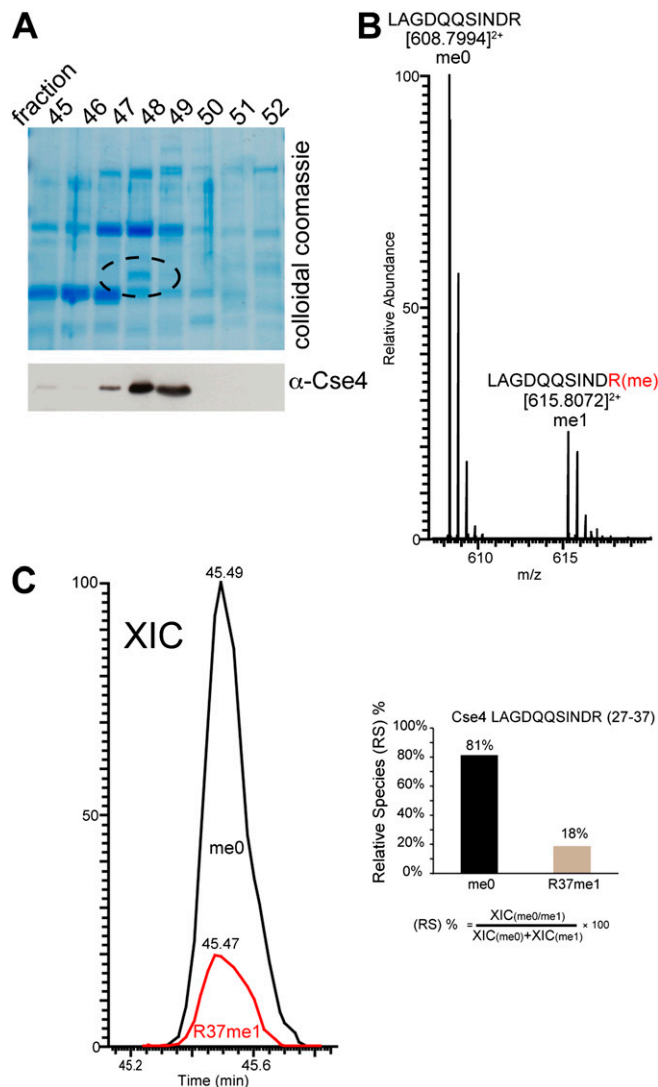


Fig. S1. Partial purification of Cse4 and estimation of relative abundance of modified Cse4 species. (A) Colloidal Coomassie-stained SDS/PAGE gel of HPLC fractions (1) of partially purified 3xHA-Cse4 were used to excise the Cse4 band (dashed circle). Cse4-containing fractions were identified by Western blotting with α -HA antibody. (B) Zoomed mass spectrum of precursor ions at m/z [608.7994]²⁺ and [615.8072]²⁺ corresponding to the unmodified (me0) and monomethylated (me1) 27-L-AGDQQSIND.R-37 peptide. (C) Extract ion chromatograms relative to both me0 and me1 species were used to estimate the relative abundance of the two species, as reported in the formula (Right).

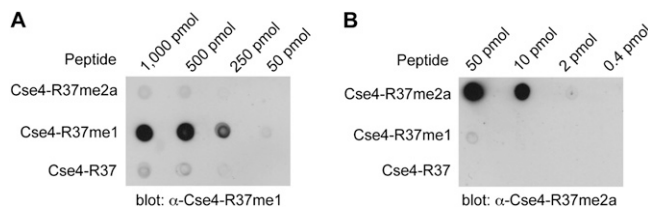


Fig. S2. Specificity of Cse4 R37me1 and R37me2a antibodies. (A) Immunodot blot showing the specific reactivity of the Cse4-R37me1 antibody. The indicated amounts of modified and unmodified peptides were spotted on nitrocellulose membrane and probed against α -Cse4-R37me1 (1:200). (B) Specificity of the Cse4-R37me2a antibody. Immunodot blot was performed as in A and probed against α -Cse4-R37me2a (1:200).

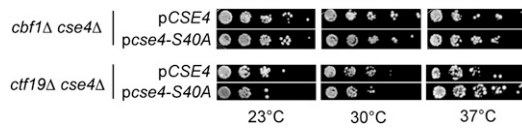


Fig. S3. Mutation of serine 40 within the essential N-terminal domain of Cse4 (*cse4-S40A*) did not cause a synthetic growth defect in *cbf1Δ* or *ctf19Δ* cells. Plasmid-borne *cse4-S40A* was introduced into *cse4Δ* strains deleted for *CBF1* or *CTF19*, and serial dilutions of the strains were spotted on complete medium and incubated at the indicated temperatures.

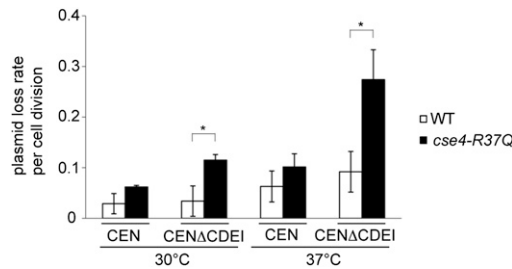


Fig. S4. *cse4-R37Q* showed a maintenance defect for plasmids lacking the centromere DNA element I (CDEI) sequence of CEN6. Error bars give SD of three independent experiments. *Significant difference, $P < 0.01$.

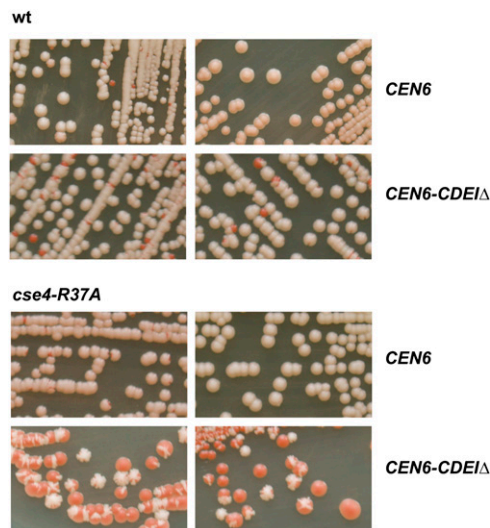


Fig. S5. *cse4-R37A* caused the loss of chromosome fragments carrying a mutation of CDEI in CEN6. Diploid strains that were either WT for *CSE4* or homozygous for *cse4-R37A* were generated that contained a large chromosomal fragment marked with *URA3* and *SUP11* and carried either CEN6 or CEN6-CDEIΔ (8). Loss of this artificial chromosome during nonselective growth could be monitored visually by colony color, because *SUP11* suppresses the *ade2-101* allele present in these strains.

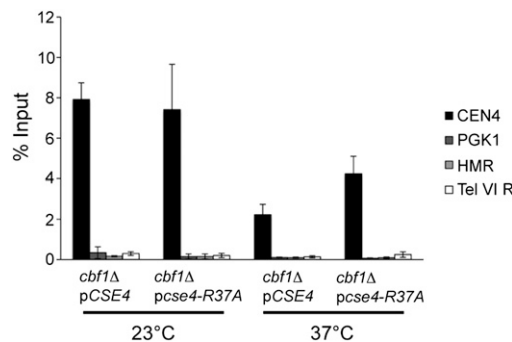


Fig. S6. Cse4 was not stabilized at noncentromeric loci. The association of Cse4 at CEN4, *PGK1*, *HMR*, and TEL-VI R was measured by ChIP. Analysis and representation are as in Fig. 4A.

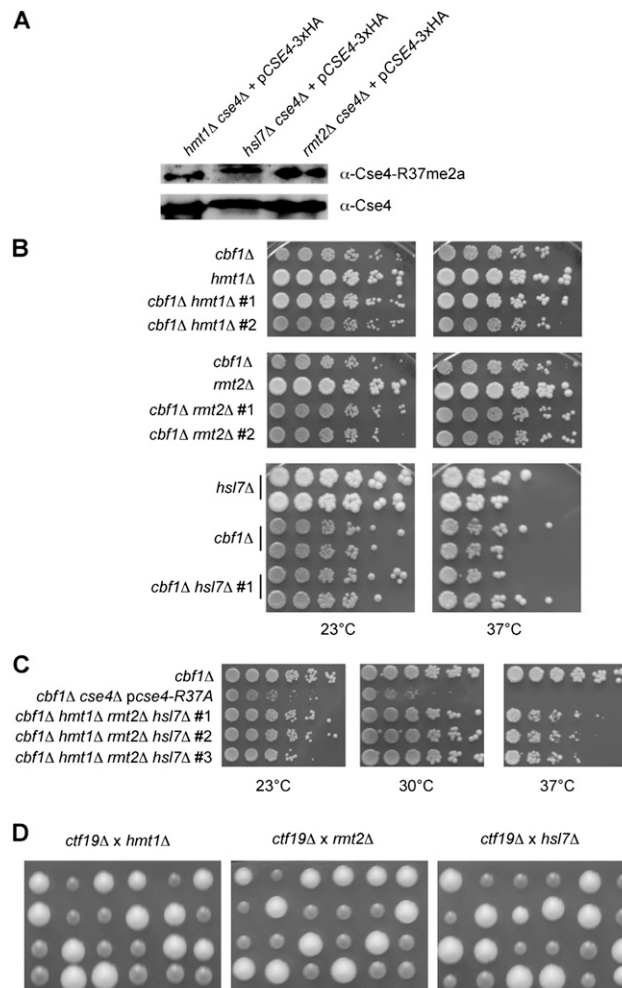


Fig. S7. The annotated arginine methyltransferases Hmt1, Hsl7, and Rmt2 were not responsible for Cse4-R37 methylation. (A) Deletion of genes encoding arginine methyltransferases did not cause a loss of asymmetrical dimethylation of Cse4 R37. Histone extracts were probed with the α -Cse4-R37me2a antibody. Cse4-3xHA was detected with α -HA as a loading control. The decrease of Cse4-R37me2a signal in the *hsl7Δ* strain was due to a lower amount of total Cse4 in the preparation. (B) Deletion of *HMT1*, *RMT2*, and *HSL7* did not cause growth defects and synthetic lethality in the absence of Cbf1. Serial dilutions of segregants from crosses between *cbf1Δ* (AEY4816) and *hmt1Δ* (AEY4818), *rmt2Δ* (AEY4820) or *hsl7Δ* (AEY4822) were spotted on full medium and incubated for five days at the indicated temperatures. The top rows show the parental strains. (C) Simultaneous absence of the annotated arginine methyltransferases did not cause a synthetic growth defect in *cbf1Δ*. Serial dilutions of *cbf1Δ* (AEY4816), *cbf1Δ cse4Δ pcse4-R37A* (AEY4848) and three *cbf1Δ hmt1Δ rmt2Δ hsl7Δ* strains (AEY4931) were spotted on full medium and incubated for three days at indicated temperatures. (D) Deletion of annotated arginine methyltransferases in *ctf19Δ* cells revealed no synthetic lethality. Tetrad dissection of genetic crosses between *ctf19Δ* and the indicated deletions are shown. The four spores from individual asci are aligned in vertical rows and were incubated at 30 °C.

Table S1. *S. cerevisiae* strains used in this study

Strain	Genotype	Source*
AEY1	<i>MATα ade2-101 his3-11,15 trp1-1 leu2-3,112 ura3-1</i> (W303)	J. Rine (University of California, Berkeley, CA)
AEY2	AEY1, but <i>MATα</i>	J. Rine
AEY3	AEY1, but <i>ADE2 lys2Δ</i>	J. Rine
AEY4	AEY2, but <i>ADE2 lys2Δ</i>	J. Rine
AEY7	<i>MATα/MATα HMRα/HMR-ssΔI</i> , W303 (diploid)	
AEY685	<i>MATα HMRα-e** cin8Δ::LEU2 ade2 LYS2</i>	
AEY2781	<i>MATα cse4Δ::KanMX ade2 lys2 + pRS426-3xHA-CSE4</i>	
AEY2797	<i>MATα cep3-2</i> , W303 (SBY162)	S. Biggins (Fred Hutchinson Cancer Research Center, Seattle, WA)
AEY2799	<i>MATα ndc10-1</i> , W303 (SBY164)	S. Biggins
AEY2800	<i>MATα ndc10-2</i> , W303 (SBY165)	S. Biggins
AEY2801	<i>MATα cep3-1</i> , W303 (SBY168)	S. Biggins
AEY2802	<i>MATα mif2-3 leu2 trp1 ura3 ADE2 LYS2 HIS3</i>	L. Hartwell (Fred Hutchinson Cancer Research Center, Seattle, WA)
AEY4816	AEY1 <i>cbf1Δ::NatMX</i>	
AEY4818	AEY4 <i>hmt1Δ::kanMX</i>	
AEY4820	AEY4 <i>rmt2Δ::kanMX</i>	
AEY4822	AEY4 <i>hsl7Δ::kanMX</i>	
AEY4846	<i>MATα cse4Δ::KanMX cbf1Δ::NatMX</i> , W303, <i>ade2 lys2 + pRS313-3xHA-CSE4</i>	
AEY4848	<i>MATα cse4Δ::KanMX cbf1Δ::NatMX</i> , W303, <i>ade2 lys2 + pRS313-3xHA-cse4-R37A</i>	
AEY4854	<i>MATα cbf1Δ::NatMX hsl7Δ::KanMX ade2 LYS2</i> , W303	
AEY4855	<i>MATα cbf1Δ::NatMX hsl7Δ::KanMX ade2 lys2</i> , W303	
AEY4856	<i>MATα cbf1Δ::NatMX hmt1Δ::KanMX ade2 lys2</i> , W303	
AEY4857	<i>MATα cbf1Δ::NatMX hmt1Δ::KanMX ade2 LYS2</i> , W303	
AEY4858	<i>MATα cbf1Δ::NatMX rmt2Δ::KanMX ade2 LYS2</i> , W303	
AEY4859	<i>MATα cbf1Δ::NatMX rmt2Δ::KanMX ade2 LYS2</i> , W303	
AEY4874	AEY4858 <i>hsl7Δ::HISMX</i>	
AEY4880	<i>MATα ade2-101 trp1-Δ63 leu2-Δ1 ura3-52 his3-Δ200 lys2-801 mcm21Δ::TRP1</i>	J. Lechner (University of Heidelberg, Heidelberg, Germany)
AEY4881	<i>MATα ade2-101 trp1-Δ63 leu2-Δ1 ura3-52 his3-Δ200 lys2-801 okp1-5Δ::TRP1</i>	J. Lechner
AEY4917	<i>MATα csm3Δ::KanMX</i> , W303	A. Marston (University of Edinburgh, Edinburgh, UK)
AEY4918	<i>MATα iml3Δ::KanMX</i> , W303	A. Marston
AEY4919	<i>MATα chl4Δ::KanMX</i> , W303	A. Marston
AEY4920	<i>MATα ctf3Δ::KanMX</i> , W303	A. Marston
AEY4921	<i>MATα mtw1-11 ade2-1 trp1-1 can1-100 leu2-3,112 his3-11,15 ura3 ssd1</i>	J. Kilmartin (Medical Research Council Laboratory of Molecular Biology, Cambridge, UK)
AEY4922	<i>MATα ndc80-1 ade2-1 trp1-1 can1-100 leu2-3,112 his3-11,15 ura3 ssd1</i>	J. Kilmartin
AEY4923	<i>MATα spc24-1 ade2-1 trp1-1 can1-100 leu2-3,112 his3-11,15 ura3 ssd1</i>	J. Kilmartin
AEY4924	<i>MATα spc25-1 ade2-1 trp1-1 can1-100 leu2-3,112 his3-11,15 ura3 ssd1</i>	J. Kilmartin
AEY4925	<i>MATα spc105-4 ade2-1 trp1-1 can1-100 leu2-3,112 his3-11,15 ura3 ssd1</i>	J. Kilmartin
AEY4931	AEY4874 <i>hmt1Δ::URAMX</i>	
AEY4946	<i>MATα ame1-4::TRP1</i> , W303, <i>ade2 lys2</i>	J. Vogel (McGill University, Montreal, Canada)
AEY4965	AEY4 <i>cse4-R37A</i>	
AEY4974	AEY1 <i>ctf19Δ::KanMX</i>	
AEY4983	AEY3 <i>cse4-R37A</i>	
AEY4985	<i>MATα cse4-R37A cbf1Δ::NatMX ADE2 LYS2</i> , W303	
AEY4990	AEY2 <i>cse4-R37A iml3Δ::KanMX</i>	
AEY5005	<i>MATα/MATα cse4-R37A/cse4-R37A</i> , W303 (diploid), <i>lys2Δ/LYS2</i>	
AEY5040	<i>MATα cse4Δ::KanMX ade2 lys2</i> , W303 + <i>pRS423-3xHA-cse4-R37A</i>	
AEY5083	AEY1 <i>ctf19Δ::NatMX</i>	
AEY5165	<i>MATα cbf1Δ::NatMX MTW1-9xmyc-KanMX cse4-R37A ade2 LYS2</i> , W303	
AEY5166	<i>MATα cbf1Δ::NatMX MTW1-9xmyc-KanMX ade2 LYS2</i> , W303	

Table S1. Cont.

Strain	Genotype	Source*
AEY5173	<i>MAT</i> α <i>cbf1</i> Δ ::NatMX <i>AME1</i> -9xmyc-KanMX <i>ADE2</i> <i>LYS2</i> , W303	
AEY5174	<i>MAT</i> α <i>cbf1</i> Δ ::NatMX <i>MTW1</i> -9xmyc-KanMX <i>cse4-R37A</i> <i>ade2</i> <i>LYS2</i> , W303	
AEY5194	<i>MAT</i> α <i>cse4</i> Δ ::KanMX <i>cbf1</i> Δ ::NatMX <i>ade2</i> <i>lys2</i> , W303 + pRS313	
AEY5195	<i>MAT</i> α <i>cse4</i> Δ ::KanMX <i>cbf1</i> Δ ::NatMX <i>ade2</i> <i>lys2</i> , W303 + pRS313-3xHA-CSE4-R37A	
AEY5254	AEY2781 <i>rmt2</i> Δ ::NatMX	
AEY5256	AEY2781 <i>hmt1</i> Δ ::NatMX	
AEY5266	AEY2781 <i>hsl7</i> Δ ::NatMX	
AEY5297	AEY4 <i>cse4-R37Q</i>	

*Unless indicated otherwise, strains were generated in this study or are from the laboratory collection. All strains except for AEY2802 are isogenic to W303.

Table S2. Plasmids used in this study

Plasmid	Description	Source*
pRS313	CEN6, <i>HIS3</i>	(1)
pRS414	CEN6, <i>TRP1</i>	(1)
pAE615	pRS313-3xHA-CSE4 [†]	
pAE977	pRS426-3xHA-CSE4	
pAE1579	pRS313-3xHA- <i>cse4-R37A</i>	
pAE1636	pRS306- <i>cse4-R37A</i>	
pAE1755	pRS423-3xHA- <i>cse4-R37A</i>	
pAE1768	<i>URA3</i> , <i>ARS3</i> , <i>SUP11</i> , <i>TEL</i> , <i>CEN6</i> <i>CDE1</i> Δ (pYCF5/d66)	P. Hieter (University of British Columbia, Vancouver, Canada; ref. 2)
pAE1769	<i>URA3</i> , <i>ARS3</i> , <i>SUP11</i> , <i>TEL</i> (pYCF5)	P. Hieter (2)
pAE1771	<i>TRP1</i> , <i>ARS1</i> , <i>CEN6</i> - <i>CDE1</i> Δ (d66)	P. Hieter (3)
pAE1847	pRS313-3xHA- <i>cse4-S40A</i>	
pAE1867	pRS313-3xHA- <i>cse4-R37Q</i>	

*Unless indicated otherwise, plasmids were generated in this study. Cloning details are available upon request.

[†]3xHA was inserted into a natural XbaI restriction site within *CSE4* that placed the tag between amino acids 81 and 82 of Cse4, analogous to ref. 4.

1. Sikorski RS, Hieter P (1989) A system of shuttle vectors and yeast host strains designed for efficient manipulation of DNA in *Saccharomyces cerevisiae*. *Genetics* 122:19–27.
2. Hegemann JH, Shero JH, Cottarel G, Philippsen P, Hieter P (1988) Mutational analysis of centromere DNA from chromosome VI of *Saccharomyces cerevisiae*. *Mol Cell Biol* 8:2523–2535.
3. Panzeri L, Landonio L, Stotz A, Philippsen P (1985) Role of conserved sequence elements in yeast centromere DNA. *EMBO J* 4:1867–1874.
4. Stoler S, Keith KC, Curnick KE, Fitzgerald-Hayes M (1995) A mutation in *CSE4*, an essential gene encoding a novel chromatin-associated protein in yeast, causes chromosome nondisjunction and cell cycle arrest at mitosis. *Genes Dev* 9:573–586.